Iranian Reasearch Organization for Science and Technology (IROST)

Advances in Environmental Technology 1 (2021) 19-27

Advances in Environmental Technology

Journal home page: https://aet.irost.ir/

# Surface Ignition using ethanol on Mo and $Al_2O_3$-$TiO_2$ coated in CI engine for environmental benefits

**Ramanujam Soundararaj[1*], Joseph Raj Francis Xavier[2], Rajendiran Ramadoss[3], Pandian Balu[4], Veerasundaram Jayaseelan[5]**

*[1*]Department of Mechanical Engineering, Mailam Engineering College, Mailam, India*

*[2] School of Mechanical Engineering, VIT Bhopal University, Bhopal, Madhya Pradesh, India*

*[3]Department of Mechanical Engineering, SRM Easwari Engineering College, Ramapuram, Chennai, India*

*[4]Department of Automobile Engineering, Bharath Institute of Higher Education and Research, Chennai, Tamil Nadu, India*

*[5]Department of Mechanical Engineering, Prathyusha Engineering College, Chennai, India*

**ARTICLE INFO**

*Article history:*
Received 25 December 2020
Received in revised form
28 August 2021
Accepted 28 August 2021

**Keywords:**
Molybdenum (Mo)
$Al_2O_3$+$TiO_2$
Low heat rejection engines
Surface ignition
Glow plug

**ABSTRACT**

Today, because of expansion in oil costs, restricted petroleum product assets, ecological thought and an unnatural weather change, the ethanol fills have been centered around elective powers. The use of ethanol is more effective in compression ignition (CI) engines because it is about 30 percent more effective than in spark-ignition (SI) engines due to increased combustion efficiency. The use of ethanol in low heat rejection (LHR) engines helps raise the temperature of the combustion chamber, creating a heat barrier around it. The effect of coating the cylinder head, pistons, and valves of a diesel engine with the molybdenum (Mo) and $Al_2O_3$+$TiO_2$ is investigated in this work. As a result, the coated pieces of the combustion chamber were accommodated by a heated boundary. The coated and uncoated engines were evaluated under similar engine operating conditions. The CO, HC, and smoke emissions were reduced, but NOx emissions slightly increased for the $Al_2O_3$+$TiO_2$ coated engine. As a result, it has the most beneficial environmental effects. (VOCs). $PM_{2.5}$ showed a positive correlation with $PM_{10}$ ($R^2$=0.84), indicating that both $PM_{2.5}$ and $PM_{10}$ were produced from similar pathways of fossil fuel combustion by automobiles and industrial activities. Further, the air quality index (AQI) analysis showed unhealthy atmospheric conditions throughout the year for city dwellers around the study area.

*Corresponding author
E-mail: balumitauto@gmail.com
DOI: 10.22104/AET.2021.4591.1261

## 1. Introduction

The vehicle worldwide energy crises, the need for improved engine strength and performance, and stricter standards to reduce emissions has encouraged all nations in the quest for elective fuel sources. One possible elective fuel source, is ethanol. Heat boundary coating is used to improve the potential for doing more work by lowering losses. Heat barrier coating on the cylinder crown surface prompts a decrease in fuel consumption and heat rejection in the coolant by improving the performance [1]. By reducing heat loss due to environmental factors, the CI engine's heat productivity increases. Protecting the cylinder head, chamber head, and valves can limit heat loss. These types of engines are referred to as LHR engines [2]. Because the coating materials have low heat transfer, the heat transition into the cylinder is reduced, and thus heat transmission to the coolant is reduced. Thermal barrier coated engines ensure increased heat productivity and a reduced primary cooling system [3]. Thermal barrier coatings are used not only for minimizing in-chamber heat dismissal and heat weariness protection of basic metallic surfaces, but also for the potential reduction of engine emissions like smoke, CO, and HC [4]. It was thought that the best and most cost-effective strategy to cope with increasing the exhibition, burning, and decreasing in discharge was to utilize an ideal covering thickness of 500 µm and a minimum covering thickness of 120 µm. If it exceeds the appropriate thickness range, the temperature of the combustion chamber separator rises to higher quality, reducing volumetric efficiency, causing a lack of oil, and decreasing heat proficiency [5]. Thermal barrier coating enables the use of low cetane value and high latent heat of vaporization of ethanol to reduce the fuel's start delay. Because of the burning time, the emission of unburned hydrocarbons in the LHR is likely to decrease. The expansion in the temperature in the burning chamber causes a slight abatement in the carbon monoxide outflow [6]. Anhydrous ethanol contains no more than 0.7 percent water by weight, but hydrous ethanol contains up to 7.4 percent water by weight at 200°C Ethanol cannot be blended with diesel in an ethanol diesel mix or emulsion without the consistency of an added substance. The heat productivity of the engine relies upon the ethanol diesel mix and the property of fuel mix in contrast with the unadulterated diesel [7]. Ethanol mix is effectively dissipated because of high chamber temperature which happens when utilizing heat boundary coating [8]. As the oxygen concentration of the ethanol mix increases, the adiabatic fire temperature decreases linearly, and thus NOx decreases even in the heat boundary coated engine [9,10]. The objective of this work is to replace diesel with pure ethanol in a modified (surface ignition) diesel engine; furthermore, an investigation was performed on an LHR with coated Mo and $Al_2O_3$+$TiO_2$.

## 2. Methods and materials

### *2.1. Modification of cylinder head and coating*

In addition to the fuel injector, a glow plug is installed in the engine cylinder head to facilitate the ignition of the combustion charge. For securing the glow plug, a bush was placed in the cylinder head after an internal thread was created in it. The glow plug was placed in the space designated for the fuel injector to create the pre-combustion chamber, allowing for quick flame propagation and smooth combustion. $Al_2O_3$+$TiO_2$ was infused into an extremely hot plasma fire, where it was rapidly heated and accelerated to a high speed. Plasma showering was accomplished by maintaining an electric curve in the spout and using a terminal as a heat source. This curve rapidly heated the surge of inactive gases that exited the chamber. The high temperature separated and ionized the gas atoms. The covering material was infused into the powder structure via a transporter gas from the feed unit.

### *2.2. Scanning electron microscope analysis*

The micrograph of the break surface of the $Al_2O_3$ + $TiO_2$ coated cylinders crown is shown in Figure 1. It demonstrates that the particles of the two materials were bent and softened on the cylinder head surface as a result of the plasma showering effect. The overall appearance of the coating was helpful in identifying the little fractures and oxidation. The structure of the top layer of the $Al_2O_3$ + $TiO_2$layer displayed porosity, few voids, oxide incorporation, unmelted particles, and breaks of miniature size. The high porosity attributes of $Al_2O_3$

+ $TiO_2$added to the fragility of the structure [11,12]. There was a significant difference between the microstructures of the covering material and the bond covering. This could be an explanation for LHR causing a decrease in heat movement [13]. This might be the cause of inadequate heat proficiency, and the heat will be lost through the engine's coated piece's breaks in this state of a few microscopic breaks. This will undermine the encouragement to coat [14].

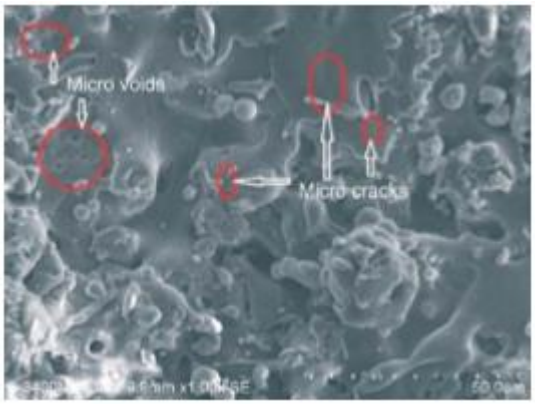


**Fig. 1.** The SEM micrographs of $Al_2O_3$ + $TiO_2$ coated surface.

*2.3. Experimental work*

Figure 2 depicts the experimental setup used in this study, and Table 1 contains the specifications. The engine's evaluated injection weight was 200bar, and the static injection timing was 23° BTDC. Before starting the engine, the fuel levels, a stream of cooling water, and the grease oil levels in the engine oil sump were all checked. The speed of the engine was maintained at the estimated speed. By estimating the current and voltage, the force created by the engine was determined. To quantify the cooling water temperature, a thermocouple was used with an advanced temperature marker. A piezoelectric weight sensor estimated the chamber pressure. QROTECH gas analyzers estimated outflows such as CO, NOx and HC. The TI Diesel Tune smoke meter was used to quantify the discharged fumes [15].

**Table 1.** Specification of the engine.

| | | |
|---|---|---|
| Make and model | : | Kirloskar, TAF 1 |
| Common Details | : | Four stroke, Compression Ignition, water-cooled. |
| Rated output | : | 4.4 kW at 1500 rpm |
| Bore | : | 80mm |
| Stroke | : | 110 mm |
| Number of cylinders | : | One |
| Clearance volume | : | 36.87 cc |
| Swept volume | : | 553 cc |
| Compression ratio | : | 16.5:1 |

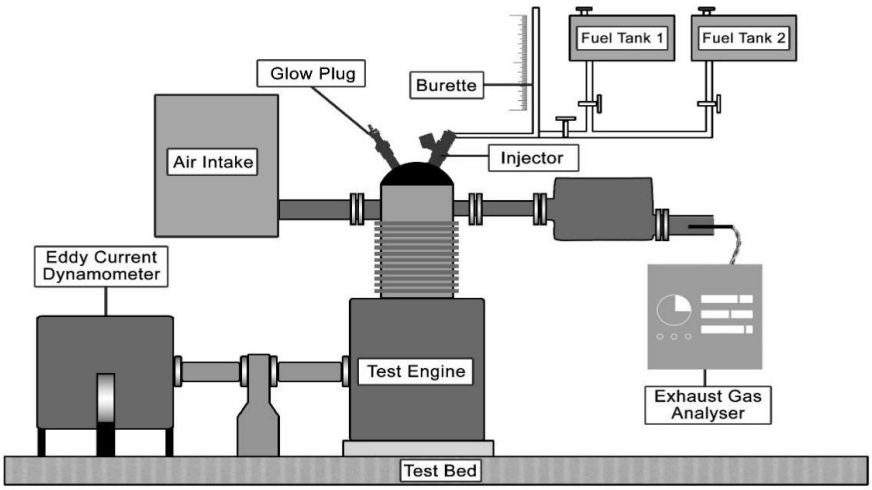


**Fig.2.** Experiment set up.

## 3. Results and discussions

### *3.1. Brake thermal efficiency (BTE)*

Figure 3 shows the variety of BTE for brake power for the standard and LHR engine. The figure shows that the BTE of ethanol with $Al_2O_3$+$TiO_2$ higher loads is 24.62, 26.2 and 29.56%, respectively, for the standard engine, molybdenum, and $Al_2O_3$+$TiO_2$ with ceramic coatings. It is well known that LHR engines covered with the $Al_2O_3$+$TiO_2$ BTE outperformed the others because the ceramic coating acts as a barrier to heat transfer from the engine to the environment. The decrease in thermal efficiency eventually expanded the influence yield and heat productivity of the engine [16].

### *3.2. Brake Specific Energy Consumption (BSEC)*

Figure 4 depicts the variation of BSEC Vs brake power for conventional coated Molybdenum (Mo) and $Al_2O_3$+$TiO_2$ materials. The BSEC was very high with little load activity and low for higher loads. At maximum load, the BSEC of the ethanol-powered Molybdenum (Mo) and $Al_2O_3$+$TiO_2$ engines was increased by 6.21 and 1.956 percent, respectively, as compared to the diesel engine. Heat energy that was exhausted outside and used for cooling was reduced in the LHR engine as a result of the coating, which improved combustion [4].

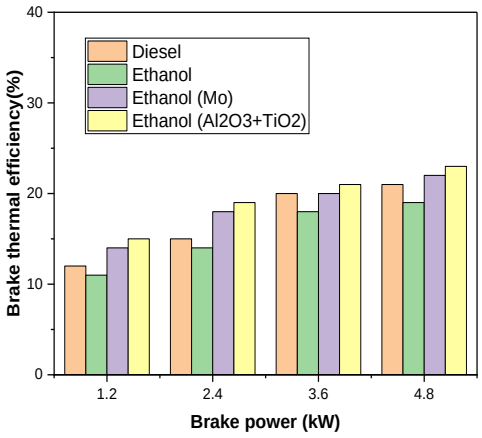


**Fig. 3.** Brake power vs brake thermal efficiency.

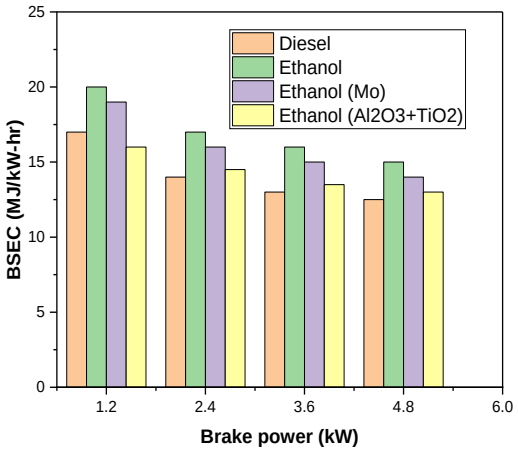


**Fig.4.** Brake power vs brake specific energy consumption.

### *3.3. Exhaust Gas Temperature (EGT)*

Figure 5 depicts the variation in EGT with respect to brake power for the conventional and LHR engines. At the most extreme load, the EGT of the ethanol-filled Molybdenum (Mo) and ethanol-powered $Al2O_3$+$TiO_2$ engines was expanded by 23.43 percent and 12.52 percent, respectively, when compared to the ethanol-energized uncoated engine with the diesel engine. In coated engines, the temperature of the emissions is higher than in uncoated engines due to a reduction in heat losses into the cooling framework [17].

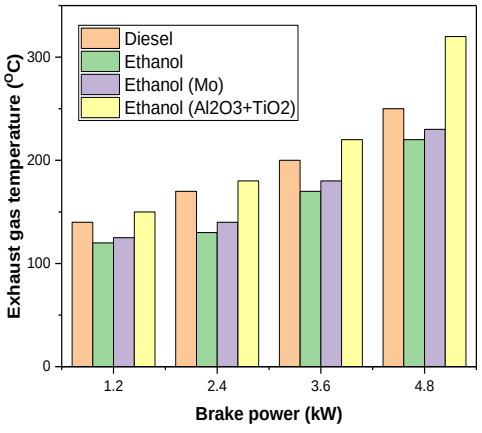


**Fig. 5.** Brake power vs exhaust gas temperature.

### *3.4. Carbon monoxide (CO) emission*

Figure 6 illustrates the relationship between the CO and brake power. As can be shown, when compared to the ethanol-powered uncoated engine, the CO emissions of the ethanol-powered

Molybdenum (Mo) and ethanol-filled $Al_2O_3$+$TiO_2$ engines were reduced by 15.52 percent and 27.46 percent, respectively. Because of the increased ignition chamber temperature induced by the protection, vaporization is improved, resulting in superior ethanol blending [18].

### *3.5. Unburnt hydrocarbon (UBHC) emission*

Figure 7 depicts the relationship between UBHC and brake power. When compared to the ethanol-fueled uncoated engine, the UBHC emission from the ethanol-fueled Molybdenum (Mo) and ethanol-fueled $Al_2O_3$+$TiO_2$ engines was reduced by 12.55 percent and 6.02 percent, respectively, at higher loads. This reduction in UBHC emissions in the coated engine would be caused by an increase in after-ignition temperature due to the reduced heat rejection to cooling, resulting in the addition of more UBHC to the burning [19].

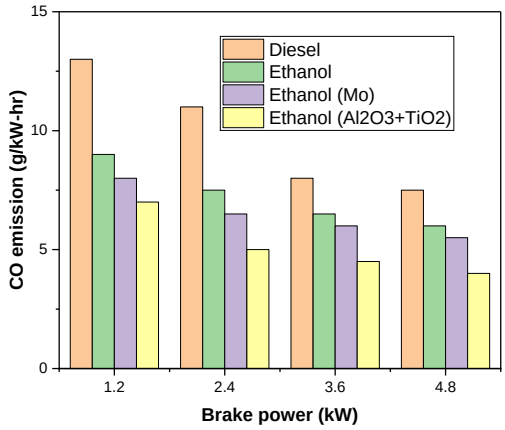


**Fig. 6.** Brake power vs CO emission.

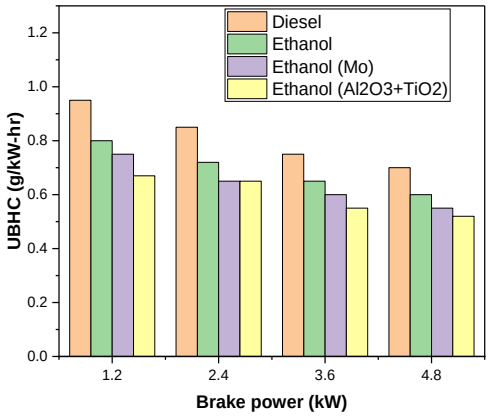


**Fig. 7.** Brake power vs UBHC emission.

### *3.6. Nitrogen oxide (NOx) emission*

Figure 8 depicts the variation of NOx in relation to brake power for standard and LHR engines. When compared to the ethanol-powered uncoated engine with conventional injection timing, the NOx outflow of the ethanol-filled Molybdenum (Mo) and ethanol-energized $Al_2O_3$+$TiO_2$ engines increased by 5.21 and 17.33 percent, respectively. The coating extending after ignition could be due to higher NOx emissions from the coated engine [19].

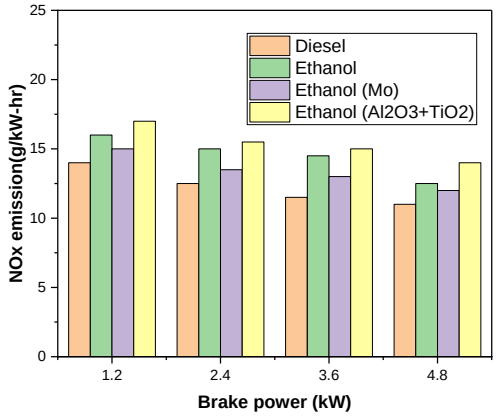


**Fig. 8.** Brake power vs NOx emission.

### *3.7. Smoke emission*

Figure 9 depicts the variation of smoke emission vs brake power for standard and LHR engines. The smoke emission of the ethanol-powered Molybdenum (Mo) and ethanol-powered $Al_2O_3$+$TiO_2$ engines was reduced by 7.26 percent and 5.10 percent, respectively, under greater loads, when compared to the ethanol-filled uncoated engine. This is a direct outcome of the greater temperature in the ignition chamber as a result of the heat boundary coating its parts. The carbon particles created by insufficient ignition frame the smoke output. Because of the greater temperatures in the ignition chamber, coating the combustion chamber's components increases ignition productivity [20].

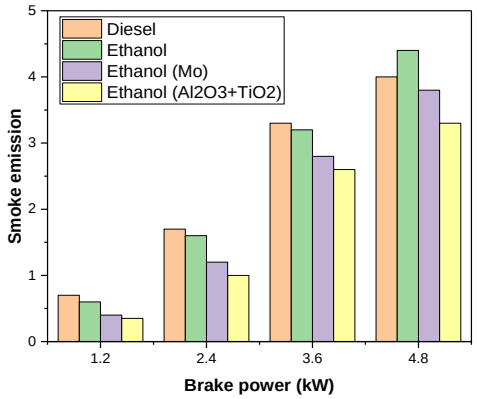


**Fig. 9.**Brake power vs smoke emission.

*3.8. Ignition delay*

Figure 10 shows the relationship between ignition delay and brake power for the standard and LHR engines. For the maximum load, the ignition delay of the Molybdenum (Mo) and ethanol-fueled $Al_2O_3$+$TiO_2$ engines is smaller than that of the ethanol-fueled uncoated engine. This is due to the hotter combustion chamber of the $Al_2O_3$+$TiO_2$ engine'. Therefore, the $Al_2O_3$+$TiO_2$ engine runs smoother compared to the conventional engine.

*3.9. Cylinder pressure*

The test results of cylinder pressure concerning the crank angle for the diesel and ethanol-fueled molybdenum (Mo) and ethanol-fueled $Al_2O_3$+$TiO_2$ engines are shown in Figure 11. The weight of the chamber relies upon the fuel's capacity to mix with air. The high weight of the chamber ensures more grounded burning and heat discharge. As the engine load rises, the pinnacle pressure increase. The higher $Al_2O_3$+$TiO_2$ engine temperature creates the greatest weight of 64.2 bar after TDC; this occurred at 12 °CA and was nearer to diesel (67.3 bar) in the CI engine. Because of the boost in temperature that hastened the in-chamber igniting measure after heat boundary coating, the most extreme weight for ethanol has been exceptionally expanded [21].

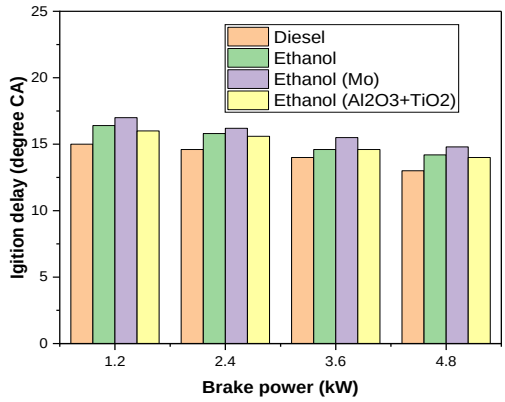


**Fig. 10.** Brake power vs ignition delay.

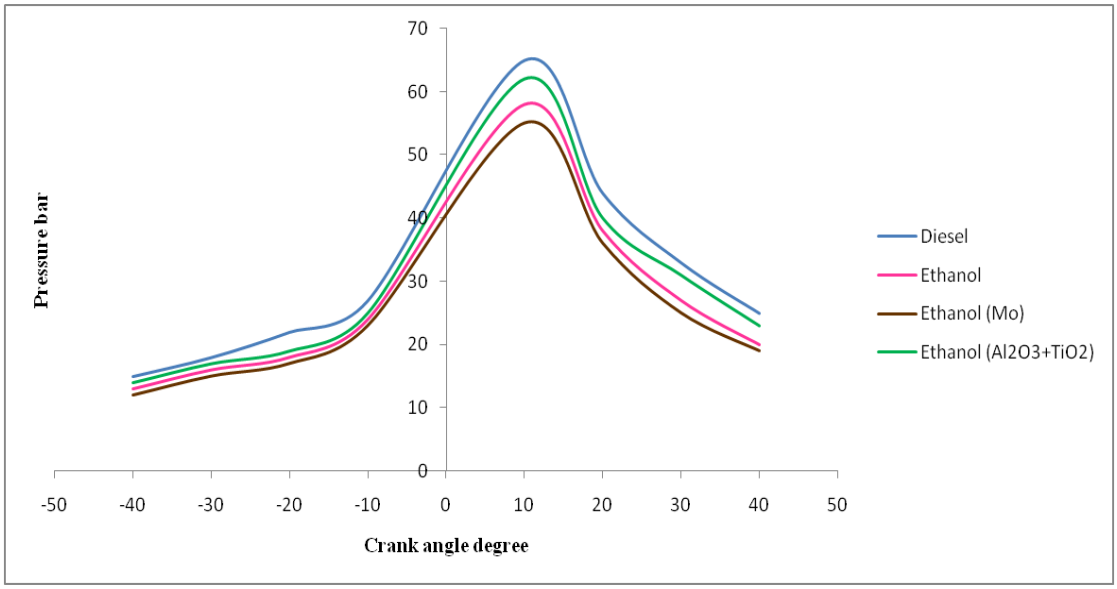


**Fig. 11.** Crank angle vs cylinder pressure.

### *3.10. Heat Release Rate (HRR)*

Figure 12 illustrates the test results for diesel and ethanol-powered Molybdenum (Mo) and ethanol-energized $Al_2O_3$+$TiO_2$ engines using HRR and crank angle. The premixed fuel-air combination consumes quickly after the start delay, followed by dispersion ignition., where the consumption rate is constrained by fuel-air blending. Because of poor atomization and the vaporization of ethanol, the HRR for ethanol was lower than that of diesel. At the maximum load, the HRR of the ethanol-filled Molybdenum (Mo) and ethanol-powered $Al_2O_3$+$TiO_2$ engines was reduced by 13.52 percent and 18.63 percent, respectively, when compared to the ethanol-powered uncoated and diesel engines.

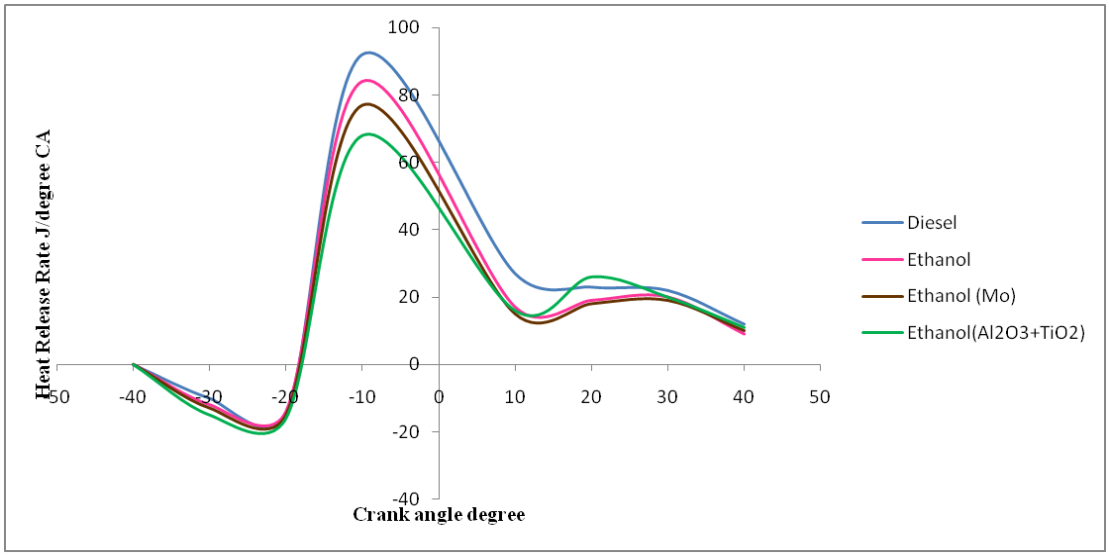


**Fig. 12.** Crank angle vs heat release rate.

## 4. Conclusions

The impact of different heat barrier coating of pottery Molybdenum (Mo) and $Al_2O_3$+$TiO_2$ on the cylinder head of ethanol were examined. The $Al_2O_3$+$TiO_2$ was used to provide superior protection, low heat rejection and a high heat coefficient. The BTE and BSEC for $Al_2O_3$+$TiO_2$ were reduced due to the ceramic coating, which impeded heat transfer from the engine to the environmental factors. CO, HC, and smoke emissions were reduced, but NOx emissions were somewhat higher in the $Al_2O_3$+$TiO_2$ coated engine. As a result, the $Al_2O_3$+$TiO_2$ coated engine provides the greatest environmental benefit.

## Nomenclature

LHR-Low Heat Rejection
Mo-Molybdenum
$Al_2O_3$+$TiO_2$-Aluminium Oxide + Titanium Oxide
TBC-Thermal Barrier Coating
CO –Carbon oxide
NOx-Oxides of Nitrogen
HC-Hydrocarbon
CI-Compression Ignition
BTDC-Before Top Dead Center
BSEC-Brake Specific Energy Consumption
EGT-Exhaust Gas Temperature
TDC-Top Dead Center
CA-Crank angle
BTE-Brake Thermal Efficiency
EGR-Exhaust Gas Recirculation

## References

[1] Vignesh, P., Kumar, A. R. P., Ganesh, N. S., Jayaseelan, V., Sudhakar, K. (2021). Biodiesel and green diesel generation: an overview. *Oil and gas science and technology–revue d'IFP energies nouvelles*, *76*, 6.

[2] Vignesh, P., Kumar, A. P., Ganesh, N. S., Jayaseelan, V., Sudhakar, K. (2020). A review of conventional and renewable biodiesel production. *Chinese journal of chemical engineering*. https://doi.org/10.1016/j.cjche.2020.10.025.

[3] Gnanamoorthi, V., Devaradjane, G. (2014). Effect of semi thermal barrier coatings on piston crown in internal combustion engine using ethanol diesel blend. *International journal of applied environmental sciences*, *9*(10), 323-332.

[4] Muthusamy, J., Venkadesan, G., Krishnavel, U. (2016). Experimental investigation of thermal barrier (8YSZ-TiO2-Al2O3) coated piston used in direct injection compression ignition engine. *Thermal science*, *20*(suppl. 4), 1189-1196.

[5] Sonoya, K., Sekine, M., Nakamura, M. (2015). Assessment of the properties of sprayed coatings for the thermal barrier applied to the piston of internal-combustion engine. *Mechanical engineering journal*, *2*(1), 14-00380.

[6] Gan, J. A., Berndt, C. C. (2015). Nanocomposite coatings: thermal spray processing, microstructure and performance. International materials reviews, 60(4), 195-244.

[7] Lawrence, P., Mathews, P. K. Deepanraj, B. (2011). Experimental Investigation on performance and emission characteristics of low heat rejection diesel engine with ethanol as fuel. *American journal of applied sciences,* 8(4), 348-354.

[8] Kaulani, S. A., Latiff, Z. A., Perang, M. R. M., Said, M. F. M., Hasan, M. F. (2019, January). Performance and emission of compression ignition (CI) engine using ethanol-diesel blending as a fuel. In *AIP conference proceedings* (Vol. 2059, No. 1, p. 020019). AIP Publishing LLC.

[9] Niculescu, R., Clenci, A., Iorga-Siman, V., Zaharia, C. (2016). Review on the Use of Bioethanol/Biomethanol—Gasoline Blends in Spark Ignition Engine. *Sci. Bul. Automot. Ser. Year XXII*, (26).

[10] Prabakaran, B., Vijayabalan, P., Balachandar, M. (2019). An assessment of diesel ethanol blend fueled diesel engine characteristics using butanol as cosolvent for optimum operating parameters. *Energy sources part A-recovery utilization and environmental effects*.UK for a range of future scenarios. *Environment international*, *61*, 36-44.

[11] Deep, A., Sandhu, S. S., Chander, S. (2017). Experimental investigations on the influence of fuel injection timing and pressure on single cylinder CI engine fueled with 20% blend of castor biodiesel in diesel. *Fuel*, *210*, 15-22.

[12] Pandey, K. K., Murugan, S. (2020). A review of bio-fuelled LHR engines. *International journal of ambient energy*, 1-24.

[13] Buyukkaya, E., Cerit, M. (2007). Thermal analysis of a ceramic coating diesel engine piston using 3-D finite element method. *Surface and coatings technology*, *202*(2), 398-402.

[14] Srikanth, H. V., Godiganur, S., Manne, B., Bharath Kumar, S., Spurthy, S. (2020). Niger seed oil biodiesel as an emulsifier in diesel–ethanol blends for compression ignition engine. *International journal of ambient energy*, 1-11.

[15] Taymaz, I., Cakir, K., Gur, M., Mimaroglu, A. (2003). Experimental investigation of heat losses in a ceramic coated diesel engine. *Surface and coatings technology*, *169*, 168-170.

[16] Subramaniam, M., Solomon, J. M., Nadanakumar, V., Anaimuthu, S., Sathyamurthy, R. (2020). Experimental investigation on performance, combustion and emission characteristics of DI diesel engine using algae as a biodiesel. *Energy reports*, *6*, 1382-1392.

[17] Najiha, M. S., Rahman, M. M., Yusoff, A. R. (2016). Environmental impacts and hazards associated with metal working fluids and recent advances in the sustainable systems: A review. *Renewable and sustainable energy reviews*, *60*, 1008-1031.

[18] Li, Y., Tang, W., Chen, Y., Liu, J., Chia-fon, F. L. (2019). Potential of acetone-butanol-ethanol (ABE) as a biofuel. *Fuel*, *242*, 673-686.

[19] Balu, P., Saravanan, P., Jayaseelan, V. (2021). Effect of ceramic coating on the performance, emission, and combustion characteristics of ethanol DI diesel engine. *Materials today: proceedings*, *39*, 1259-1264.

[20] Saravanan, P., Mala, D., Jayaseelan, V., Kumar, N. M. (2019). Experimental performance investigation of partially stabilized zirconia coated low heat rejection diesel engine with waste plastic oil as a fuel. *Energy sources, part A: recovery, utilization, and environmental effects*, 1-14.

[21] Venkatesan, B., Seeniappan, K., Shanmugam, E., Subramanian, S., Veerasundaram, J. (2021). Characterization and effect of the use of safflower methyl ester and diesel blends in the compression ignition engine. *Oil and gas science and technology–revue d'IFP energies nouvelles*, *76*, 29.